JOURNAL OF MATERIALS SCIENCE **36** (2001) 5311–5314

Combustion characteristics of WO_3/Zn reaction system in SHS process

J. H. LEE, D. H. SEO, C. W. WON
Rapidly Solidified Materials Research Center, Chungnam National University, 220 Kung-dong, Yusong-ku, Taejon, 305-764, Korea
E-mail: jong-lee@cnu.ac.kr

I. P. BOROVINSKAYA, V. I. VERSHINNIKOV
Institute of Structure Macrokinetics Russian Academy of Sciences, Chernogolovka, Moscow Region, 142432, Russia

Tungsten powder was prepared by the Self-Propagating High-Temperature Synthesis (SHS) Process of WO_3-Zn mixture. Zn vapor was discovered to affect significantly the combustion parameters such as combustion temperature (T_c), combustion velocity (U), relative mass change (Δm) and relative elongation (Δh) of the sample. These effects could be reduced by decreasing internal Ar pressure and sample density. The ZnO in the product was leached with an HCl solution. The Zinc-thermal reduction mechanism was revealed through a quenching of the sample.

1. Introduction

Tungsten has a high melting point (3410°C) as well as high-temperature strength and electrical conductivity. Thus, it finds wide applications in illumination, electronics, electrical contact and heat-resistant materials. It is also the main raw material for the hard alloys used in cutting tools, antifriction tools, and high-speed steels [1]. In industry, tungsten is usually obtained by reduction of tungsten oxide with hydrogen in furnaces with electric heat-up, because $WO_3 + H_2$ reaction is endothermic. Lately, many pure substances [2–6] including carbides [7], borides [8], intermetallic compounds [9], nitrides [10], and silicides [11] have been prepared by the self-propagating high-temperature synthesis (SHS) process using their high exothermic heats of formation. The process is relatively simple and rapid without requiring much external heat supply. That's why application of the SHS technology is one of the most promising method of tungsten powder production. Without controlling SHS process, however, required quality of products can't be provided. It is well known that the mode of combustion-front propagation divided into two large groups, gasless and gaseous combustion [12]. The former is relatively simple and has been extensively studied, whereas the heat and mass transportation phenomena of the latter is not clearly understood. Moreover, the report on the quantitative study for the gaseous combustion as of WO_3/Zn system is rare. The purpose of this study was to find out the processing parameters which govern synthesis conditions, and the effects of the such parameters as argon pressure, green mixture density, compact size and components ratio were systematically studied.

2. Experimental procedure

Powders of the following characteristics were used:

WO_3 (purity : 98.5–99.5%, particle size : less than 250 μm)
Zn (purity : 99.5%, particle size : less than 78 μm)

The green mixture was prepared in a tumbling mill for 2 hours. In order to investigate the effect of the compact density on the combustion characteristics, samples were prepared by pouring the green mixture into a paper cup or by pressing into a compact of 15–40 mm in diameter and 40 mm in height under various compaction pressure (50–300 MPa). The compacts were ignited by a tungsten coil filament. Combustion reaction was carried out in a constant pressure vessel. Combustion velocity and temperature were determined by the average value of three measurement using W-Re thermocouple (W-5Re versus W-26Re). In order to find out reaction mechanism of WO_3/Zn reaction system, the combustion front was stopped with thick wedge type copper mould. Tungsten powder with ZnO was obtained by the combustion synthesis as shown in reaction (1). Then by using 1:1 hydrochloric acid solution, the reaction product was leached. The intermediate product $3ZnO + W$ was treated with the acid for 2 hours. Soluble salts $ZnCl_2$ was washed with water using a filter, resulting pure tungsten on the filter.

$$WO_3 + 3Zn = 3ZnO + W \quad (1)$$

$$ZnO + 2HCl = ZnCl_2 + H_2O \quad (2)$$

Crystal structures of the prepared tungsten particles was studied using X-ray microanalyzer JCXA-733

"SUPERPROBE". Change of the sample length after combustion was calculated by the following equation:

$$\Delta h = \frac{h_f - h_i}{h_i} \times 100\% \tag{3}$$

where h_i and h_f were the initial and final sample length respectively.

Change of the sample mass was by the Equation 4:

$$\Delta m = \frac{m_i - m_f}{m_i} \times 100\% \tag{4}$$

where m_i and m_f were the sample initial and final weight respectively. From the change of the sample initial size and its weight loss, the effect of gas evolution on the combustion velocity and phase composition of the final product was studied.

3. Results and discussion

Fig. 1 represents the effect of argon pressure on the combustion parameters. With the pressure increase from 0.1 up to 0.8 MPa the combustion temperature increased from 1213 K up to 1343 K and then remains constant up to the pressure of 1.6 MPa. Increase of argon pressure up to 2.5 MPa results in the combustion temperature decrease to 1053 K. In the case of the further pressure increase, the combustion flame didn't self-sustained. The combustion velocity U, sample weight change Δm and elongation decreased as the Ar pressure increased, and the combustion was observed in a spin mode. It was experimentally and numerically demonstrated that the evaporation of the metal vapor is suppressed by Ar pressure. Hence, the increases of Ar pressure resulted in the decreases of the evaporation of the easily volatile component, Zn in this experiment. However, further increases of the Ar pressure resulted in the decreases of the combustion temperatures and finally the self-sustained combustion couldn't be achieved.

There may be possible explanations on this phenomena, one is that the heat removal from the sample surface becomes higher with the Ar density increase, another one is that the vaporized Zn acts as a heat transportation medium. It is clear that the sample swelling occurs due

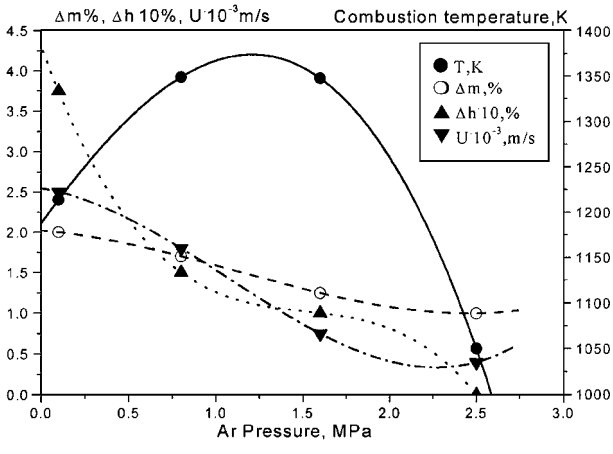

Figure 1 Effects of Ar pressure on the combustion parameters [system: $WO_3 + 3Zn$, $\rho = 2980$ kg/m^3, $d_s = 40 \times 10^{-3}$ m].

to the pressure increase in the combustion front by the formation of gas (Zn_g) and should be proportional to the difference between the gas evolution velocity (W_{ev}) and gas outlet velocity (W_o) from a unit volume of combustion zone during the combustion time, t. The volume change of the specimen during combustion reaction can be calculated on the assumption that the compact is so deformable that the evolution of the Zn vapor leads the compact to deform. If the radial swelling is negligible, overall swelling can be simplify with height change as represented by Equation 5.

$$(V_i - V_f) \approx \pi r^2 (h_i - h_f) \approx (W_{ev} - W_o)t \tag{5}$$

where V_i and V_f: initial and final volume of the specimen respectively, r: radius of the specimen, h_i and h_f: initial and final height of the specimen respectively, $W_{ev} = \rho U A V_T$, $W_o = kA/\mu \cdot \mathrm{d}P/\mathrm{d}x$—the Darcy's law [13], $t = h_i/U$, ρ: density (kg/m^3), U: combustion velocity (m/sec), A: area of the specimen (m^2), k: coefficient of the gas permeability (m^2), V_T: volume of Zn vapor per unit mass at the combustion temperature and pressure (m^3/kg), μ: dynamic viscosity of the gas (kg $\cdot$ sec/m^2); $\mathrm{d}P/\mathrm{d}x$: pressure gradient (kg $\cdot$ m^{-2}/m).

From the Equation 5

$$\pi r^2 (h_i - h_f) \approx \left(\rho U A V_T - \frac{kA}{\mu} \frac{\mathrm{d}P}{\mathrm{d}x} \right) \cdot \frac{h_i}{U} \tag{6}$$

then we divide by $\pi r^2 h_i$ and get:

$$\Delta h = \frac{h_i - h_f}{h_i} \approx \frac{\rho A V_T}{\pi r^2} - \frac{kA}{\mu} \cdot \frac{\mathrm{d}P}{\mathrm{d}x} \cdot \frac{1}{U \pi r^2}$$
$$\approx \rho V_T - \frac{k}{\mu} \cdot \frac{\mathrm{d}P}{\mathrm{d}x} \cdot \frac{1}{U} \tag{7}$$

The experimental results for the relationship between sample swelling (Δh) and Ar pressure in Fig. 1 may be explained by Equation 7, i.e. the swelling increases with V_T increases, and pressure gradient, $\mathrm{d}P/\mathrm{d}x$ decreases with argon pressure increases because the boiling temperature increases but the evaporation of the Zn vapor suppresses as the total pressure increases by Clausius-Clapeyron equation [14]. The right hand part of Equation 7 decreases with the argon pressure increases, because ρV_T is always positive, hence, it is possible to interpret that the sample swelling (Δh) decreased with the increasing of argon pressure as shown in Fig. 1.

In order to analyze the effect of the sample diameter on the combustion parameters, the subsequent experiments were realized at $P_{Ar} = 0.8$ MPa and maximum combustion temperature $T = 1343$ K as shown in Fig. 2. The combustion velocity and the temperature change were negligible, whereas the sample swelling grows from 4.9% to 14.9% as the sample diameter increases from 1.5×10^{-2} m up to 40×10^{-2} m. This can be explained by the fact that Zn vapor easily leaves the combustion front through the sample surface with decreasing of the sample diameter.

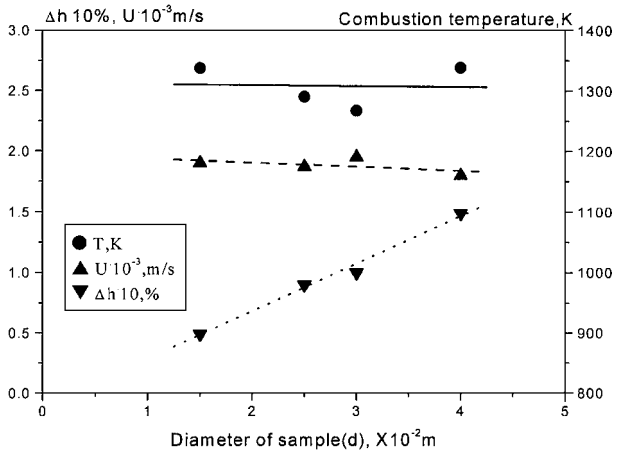

Figure 2 Effects of green pellet diameter on the combustion parameters [system: $WO_3 + 3Zn$, $\rho = 2980$ kg/m^3, $P_{Ar} = 0.8$ MPa].

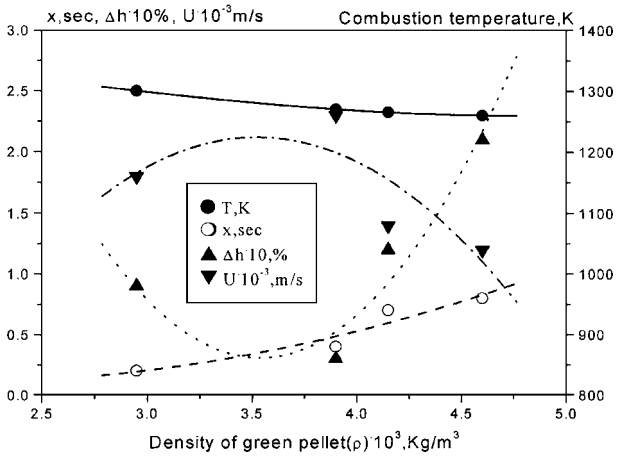

Figure 3 Effects of green pellet density on the combustion parameters (system: $WO_3 + 3Zn$, $d_s = 25 \times 10^{-3}$ m^3, $P_{Ar} = 0.8$ MPa).

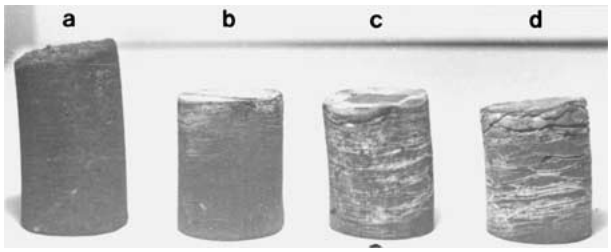

Figure 4 Burnt samples of various green density (system: $WO_3 + 3Zn$, $d_s = 25 \times 10^{-3}$ m^3, $P_{Ar} = 0.8$ MPa). (a) $\rho = 2950$ kg/m^3, (b) $\rho = 3900$ kg/m^3, (c) $\rho = 4150$ kg/m^3 and (d) $\rho = 4600$ kg/m^3.

Fig. 3 demonstrates the effect of the green density of the compact on the combustion parameters. As the green density increased from the bulk value 2950 kg/m^3 to 4600 kg/m^3, the combustion velocity decreased and the sample swelling increased. When $\rho > 4600$ kg/m^3, the combustion flame extinguished immediately after ignition. The reason of the combustion temperature decreases at dense green pellet has been accepted as the heat loss at combustion front because the effective thermal conductivity increases as the porosity decreases. In this experiment, however, both the combustion temperature and velocity may be decreased due to the decreases of the permeability.

Fig. 4 represents a photograph of the burnt samples. The sample diameter didn't change after the combustion. On the lateral surface of the samples with higher density, the traces of the spin combustion and cracks were observed. This may be because the permeability of the compacts decreased as the density increased, and then the pressurized Zn vapor boiled out from inside of the sample to the surface leaving cracks. This phenomenon also could be explained with Equation 7. The samples of $\rho = 4370$ kg/m^3 were investigated at different argon pressures and the their photographs are represented in Fig. 5.

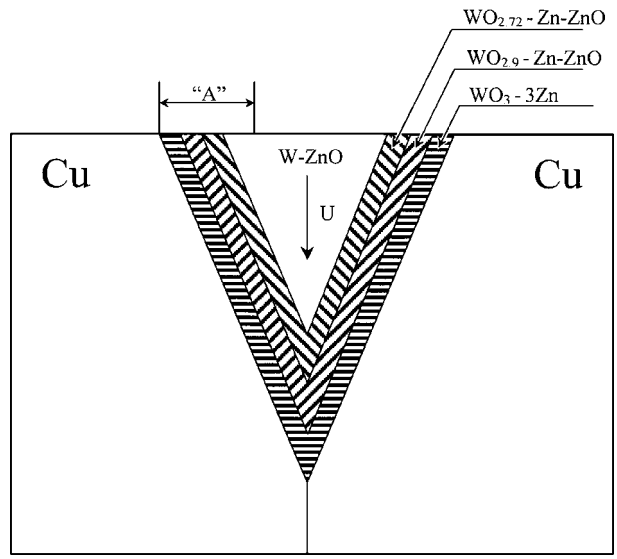

Figure 6 A scheme of sample quenching by copper mould and distribution of layers of the products (Zone "A" was treated with hydrochloric acid).

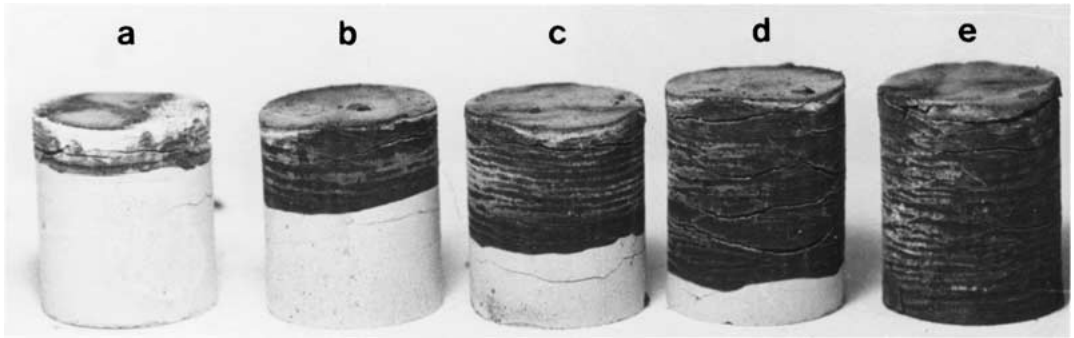

Figure 5 Photographs of the burnt samples synthesized at various Ar pressure (system: $WO_3 + 3Zn$, $d_s = 25 \times 10^{-3}$ m^3, $\rho = 4370$ kg/m^3). (a) $P_{Ar} = 1.6$ MPa, (b) $P_{Ar} = 1.4$ MPa, (c) $P_{Ar} = 1.1$ MPa, (d) $P_{Ar} = 0.96$ MPa and (e) $P_{Ar} = 0.8$ MPa.

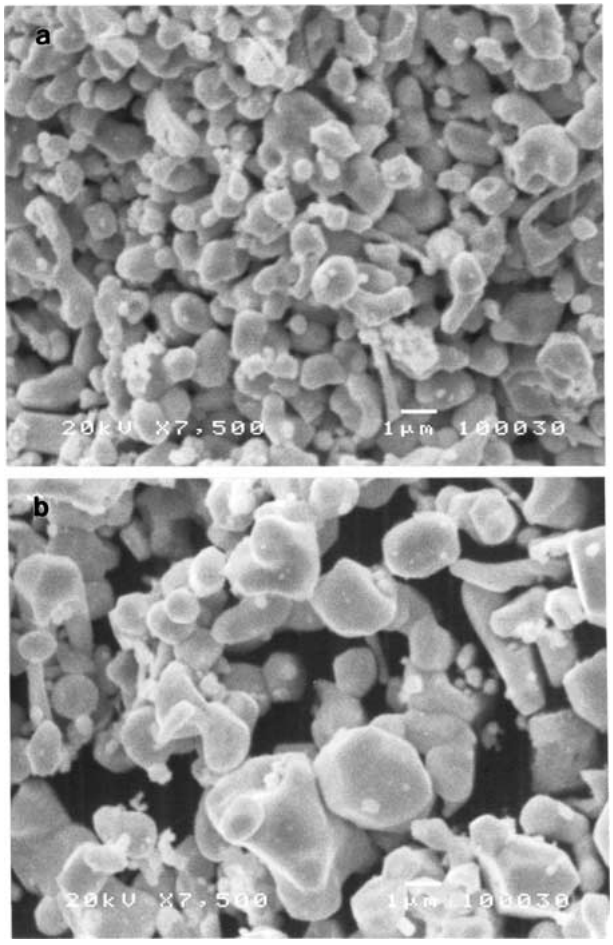

Figure 7 Effects of green pellet diameter on the W particle size [system: $WO_3 + 3Zn$, $\rho = 2980$ kg/m^3, $P_{Ar} = 0.8$ MPa]. (a) 1.5×10^{-2} m and (b) 4×10^{-2} m.

The increases of the Ar pressure from 0.8 up to 0.96 MPa caused the propagation front to be extinguished. Also, can be seen that the cracking occurred in the combusted zone as well as the front of the combustion zone. This may mean that the preheating zone was deformed by the Zn vapor.

For investigating the mechanism of zinc thermal reduction of WO_3, the combustion front was arrested in a wedge. A sample was placed in a copper mould which provided rapid heat removal from the combustion front, i.e., quenching of the sample. Layers with 4 different colors could be seen on a cut-off surface. X-ray phase analyses of the combusted samples in the copper wedge mould confirmed the existence of WO_3, $WO_{2.9} + WO_{2.72}$ and W from the mould wall to the center as shown in Fig. 6 and it was possible to conclude that the process of zinc-thermal reduction is realized in 4 stages;

1. $WO_3 + 0.1\ Zn = WO_{2.9} + 0.1\ ZnO$
2. $WO_{2.9} + 0.18\ Zn = WO_{2.72} + 0.18\ ZnO$
3. $WO_{2.72} + 0.72\ Zn = WO_2 + 0.72\ ZnO$
4. $WO_2 + 2\ Zn = W + 2\ ZnO$

As shown in Fig. 6, tungsten particle size increased as the sample diameter increased. The radial temperature gradient which determines the over cooling rate decreases as the sample diameter increases. Thus, we believe that the particle growth of the products with larger sample size resulted from the lower cooling rate.

4. Conclusions

1. Zn vapor was discovered to significantly affect the combustion parameters (Δh, Δm, U and T), also the evaporation of the zinc was suppressed as the Ar pressure increased. Hence, combustion limits by Ar pressure and sample density for the system WO_3-Zn were determined.

2. Mechanism of tungsten oxide reduction by zinc was proposed from the experimental results and modeling for the combustion procedures, and the proposed model may be adopted to the general combustion reaction system.

References

1. J. C. BAILAR and H. J. EMELEUS, *Comprehensive Inorganic Chemistry* **3** (1973) 742.
2. S. G. KO, C. W. WON, B. S. CHUN and H. Y. SOHN, *J. Mater. Res.* **10** (1995) 795.
3. S. K. KO, S. S. CHO, B. S. CHUN and C. W. WON, *Met. Trans.* **26B** (1996) 315.
4. J. C. JUNG, S. G. KO, C. W. WON, S. S. CHO and B. S. CHUN, *J. Mater. Res.* **11** (1996) 1825.
5. C. W. WON, J. C. JUNG, S. G. KO and J. H. LEE, *Mater. Res. Bull.* **34** (1999) 2239.
6. J. H. LEE, J. C. JUNG, I. P. BOROVINSKAYA, V. I. VERSHINNIKOV and C. W. WON, *Met. and Mater.* **6** (2000) 73.
7. S. K. KO, C. W. WON and I. J. SHON, *Scripta Mater.* **37** (1997) 889.
8. R. L. AXELBAUM, D. P. DUFAUX, C. A. FREY, K. F. KELTON, S. A. LAWTON, L. J. ROSEN and S. M. L. SASTRY, *J. Mater. Res.* **11** (1996) 948.
9. K. KAWASE and Z. A. MUNIR, *Int. J. SHS* **7** (1998) 95.
10. S. M. BRADSHAW and J. L. SPICER, *J. Amer. Ceram. Soc.* **82** (1999) 2293.
11. L. TAKACS, *J. Sol. Stat. Chem.* **125** (1996) 75.
12. Z. A. MUNIR and J. B. HOLT, in "Combustion and Plasma Synthesis of High-Temperature Materials," edited by Z. A. Munir and J. B. Holt (VCH Publishers, New York, 1990).
13. G. H. GEIGER and D. R. POIRIER, in "Transport Phenomena in Metallurgy" (Addison-Wesley, CA, 1973) p. 91.
14. Y. K. RAO, in "Stoichiometry and Thermodynamics of Metallurgical Processes" (Cambridge University Press, Cambridge, UK, 1985) p. 526.

Received 19 June
and accepted 3 August 2001